Math. Model. Nat. Phenom. 19 (2024) 21
https://doi.org/10.1051/mmnp/2024018

Mathematical Modelling of Natural Phenomena
www.mmnp-journal.org

MULTI-SCALE HYBRID MODELING OF PLANT GROWTH IN RESPONSE TO ENVIRONMENTAL CONDITIONS AND SOIL NUTRIENTS AVAILABILITY

Hassan Chini[1,2,*], Aissam Jebrane[1] and Abdelilah Hakim[2]

Abstract. Crop modeling plays a crucial role in agriculture, aiding our understanding and prediction of crop growth and yield in diverse environmental conditions. This study aims to develop a comprehensive mathematical model describing plant growth in response to environmental conditions and soil nutrient availability. To achieve this, we relied on a field experiment with lettuce plants under varying environmental conditions. Employing growth models such as logistic, Gompertz, Aikman & Scaife, and Scaife, Cox & Morris, we assessed the influence of time, day-degrees, and effective day-degrees across different plant densities and during distinct periods throughout the year. In general, describing plant growth in terms of day-degrees or effective day-degrees yielded an improved model fit and more precise estimations of growth parameters. As a result, we described the growth of plant length in terms of effective day-degrees instead of time in the equations of the Bessonov–Volpert system. Additionally, we modified the equation describing plant length growth using previously fitted functions. By incorporating these adjustments, we characterized the one-dimensional growth of plant weight under varying environmental conditions without branching, using the Bessonov–Volpert model. This study contributes valuable insights into crop modeling techniques, refining our understanding of optimizing plant growth under different environmental conditions.

Mathematics Subject Classification. 00A71, 92B05, 92C80.

Received February 21, 2024. Accepted September 18, 2024.

1. Introduction

Crop modeling plays a pivotal role in agriculture, serving as an indispensable tool for understanding and predicting the intricate dynamics of crop growth and yield across diverse environmental conditions and soil nutrients. The three fundamental elements crucial for plant growth—water, air, and soil—are intricately interlinked in governing processes such as photosynthesis and nutrient absorption.

Water availability is a critical determinant of plant health, influencing various physiological processes. Relevant studies [1, 2] highlight the significance of water management in optimizing crop yield.

Air, specifically carbon dioxide from the atmosphere, plays a central role in the process of photosynthesis. Researchs [2–4] underscore the importance of understanding and managing atmospheric conditions for enhanced crop productivity.

Keywords and phrases: Multi-scale modeling, plant growth, soil nutrients, environmental conditions, Bessonov–Volpert model.

[1] Centrale Casablanca, Complex Systems and Interactions Research Center, Ville Verte, Bouskoura, Morocco.
[2] LAMAI, Department of Mathematics, Faculty of Sciences and Technologies, Cadi Ayyad University, Marrakech, Morocco.

[*] Corresponding author: hassan.chini@centrale-casablanca.ma

Soil, the medium in which plants anchor their roots, provides essential nutrients vital for growth. Key components such as nitrates, phosphorus, and ammonium, along with other chemical elements, shape plant development [5, 6].

Understanding the intricate relationship between these chemical components and plant development is essential. Initially, plant modelers described plant growth in idealized environmental conditions, neglecting variations in environmental factors and soil nutrients [7–12]. However, some of these models have been extended to be applicable by introducing environmental conditions as parameters [13, 14].

To describe plant growth under variable environmental conditions more accurately, it is advantageous to consider parameters such as day-degrees (DD) or effective day-degrees (EDD). Day-degrees take into account the daily temperature, while effective day-degrees incorporate both temperature and daily radiation. Several studies, such as those conducted by Tei *et al.*[15, 16], on lettuce, onion, and red beet have demonstrated the relevance of these parameters in improving the fit and giving a better estimate of growth parameters.

Among the limitations of these models is their failure to consider soil nutrients. Other mathematical models describe plant growth in interaction with soil nutrients without taking into account environmental conditions [17–19]. For example, the Bessonov–Volpert model [20, 21] is a dynamic model that explores various growth scenarios influenced by specific parameters determined by the plant's morphology.

In this context, it's crucial to note that other models exclusively delve into root growth and its impact on agricultural yield [22, 23]. However, in our simulations, we focus solely on above-ground plant growth, excluding considerations for root growth.

Therefore, our study aims to develop a comprehensive mathematical model describing plant weight growth in response to environmental conditions and soil nutrient availability. This model will contribute valuable insights to crop modeling techniques, refining our understanding of optimizing plant growth under different environmental scenarios and fostering sustainable agricultural practices. To realize this objective, we adopt a systematic, multi-step approach.

Firstly, in Section 2.2.1, we explored various growth models, including the logistic model [24, 25], Gompertz [26], Aikman & Scaife [13], and Scaife, Cox & Morris [14]. This investigation utilized days after planting (time), day-degrees (DD), and effective day-degrees (EDD) to assess their effectiveness in portraying plant growth dynamics in response to changing environmental conditions and the competition between plants within the crop, notably influenced by plant density. As plant density increases, competition among plants intensifies, impacting soil nutrient availability and environmental conditions. This heightened competition can lead to variations in received radiation due to shading between plants, affecting overall growth dynamics and creating distinct growth patterns within the crop [27–29].

Our study rigorously evaluated these models using data obtained from lettuce experiments conducted under varied weather regimes, encompassing growth at four distinct densities (180, 480, 1920, and 7680 plants m^{-2}). This dataset allowed us to scrutinize the initial depiction of the competition effect between plants within the crop as provided by each model.

Secondly, in Section 2.2.2, our exploration extended to plant length growth in interaction with soil nutrients, employing the Bessonov–Volpert model [20, 21]. This particular model adeptly captured the evolution of plant length over time and the emergence of distinct forms influenced by plant morphology, without explicit consideration of environmental conditions.

Thirdly, in Section 2.2.3, our endeavor culminated in the development of a unified model that encapsulates both plant growth influenced by soil nutrients and environmental conditions. This involved synthesizing insights from previously examined models (logistic, Gompertz, Aikman & Scaife, and Scaife, Cox & Morris) with the Bessonov–Volpert model.

Fourthly, in Section 3.1, we commenced with the calibration of the models according to our data by examining the effects of time, day degrees, and effective day degrees. Subsequently, in Section 3.2, we transitioned to numerical simulations for the developed model using the parameters deduced from Section 3.1.

Finally, in Section 4, we initiated with a comparison of the four models to describe plant growth under variable environmental conditions. We then delved into a discussion of our model's results. This holistic approach represents a pivotal stride toward a more profound understanding of crop growth and yield prediction, ultimately contributing to the advancement of sustainable agricultural practices.

2. Materials and methods

2.1. Field experiment

Our study builds upon the experiment detailed in [14]. The experiment involved measuring average plant weights at various growth stages for four different plants: lettuce, cauliflower, celery, and leek (in our investigation, we focused exclusively on the lettuce plant). The experiment was conducted under conditions of ample water and nutrient availability.

Lettuce seeds were cultivated at four different plant densities: 180, 480, 1920, and 7680 plants m^{-2}. Three sowings occurred on the following dates: 03/09/1981, 14/10/1981, and 16/03/1982, each followed by four harvests. For example, in the case of the sowing on 03/09/1981, the harvests took place on 16/09, 22/09, 25/09, and 30/09/1981.

The coefficient of determination between the estimated and observed average weights for lettuce was found to be 99.82% (see Fig. 1 [14]). Since the observed weight values were not reported in the original article, and to estimate the parameters of our mathematical model, we considered the estimated weights as the observed weights in our study using the estimated values of a and b displayed in Appendix A, given the high coefficient of determination.

To estimate the day-degrees DD and total photosynthetically active radiation PAR at each harvest, we projected the data from Figures 3 and 4 [14] onto the x-axis. Using the equation proposed by Scaife *et al.* [14]:

$$EDD^{-1} = DD^{-1} + 0.09 \times PAR^{-1}$$

we were able to estimate the sum of PAR at each harvest, based on the DD and EDD values.

Another parameter estimated for the Scaife, Cox, and Morris model is MDR (mean daily radiation during the period of 14 days before harvest). To estimate this parameter, we projected the data from Figure 5 [12] onto the x-axis (see Appendix A).

In addition, the values obtained for each experiment's projections are presented in tabular form in the supplementary file.

2.2. Modeling

2.2.1. Modeling plant growth under varying environmental conditions

In this study, we fitted four different functions to model plant growth and predict the mean dry weight per plant (g per plant). These functions are the logistic function, the Gompertz function, the Aikman & Scaife function, and the Scaife, Cox & Morrix function. Time (t), day-degrees (DD), and effective day-degrees (EDD) were used as independent variables in the functions. The form of the functions used for plant weight, w, were as follows:

Logistic: $$w = \frac{k}{1 + \left(\frac{k}{w_0} - 1\right) \mathrm{e}^{-rx}} \tag{2.1}$$

Gompertz: $$w = a\mathrm{e}^{-b\mathrm{e}^{-cx}} \tag{2.2}$$

Aikman & Scaife: $$w = \frac{1}{dKF} \ln \left[1 + \frac{f_0}{1 - f_0} \mathrm{e}^{rx}\right] \tag{2.3}$$

Scaife, Cox & Morris: $$w^{-1} = w_0^{-1} \mathrm{e}^{-rx} + q^{-1} MDR^{-1} d \tag{2.4}$$

Table 1. Parameters and definitions used in the models.

Notation	Description	Unit
w	Mean dry weight per plant excluding fibrous roots	$\mathrm{g\,p^{-1}}$
w_0	Mean dry weight per plant at the first sampling, *i.e.* at $x = 0$	$\mathrm{g\,p^{-1}}$
t	Days from sowing	days
x	A variable represents time (t), day degrees (DD) or effective day degrees (EDD)	days, °C
r	Early relative growth rate per x for logistic model	x^{-1}
c	Early relative growth rate per x for Gomoertz model	x^{-1}
k	Carrying capacity for the logistic model	$\mathrm{g\,p^{-1}}$
a	Carrying capacity for the Gompertz model	$\mathrm{g\,p^{-1}}$
b	The displacement along the x-axis $\left(= ln(\frac{w_O}{k})\right)$	–
d	Plant density	$\mathrm{g\,m^{-2}}$
l	Mean leaf area per plant	$\mathrm{m^2\,p^{-1}}$
K	Light extinction coefficient	–
q	A proportionality constant relating the ceiling yield to MDR	$\mathrm{m^4\,g^{-1}\,MJ^{-1}}$
F	Leaf area ratio	$\mathrm{m^2\,g^{-1}}$
f	Fraction of light intercepted by the leaf area ($\mathrm{PAR_{intercepted}/PAR_{incident}}$)	–
LAI	Leaf area Index	$\mathrm{m^2(leaves)/m^2(ground)}$
MDR	Mean daily photosynthetically active radiation for 14 days before to harvest	$\mathrm{MJ\,m^{-2}}$

The commonly used approach for estimating the fraction f of incident radiation intercepted by foliage involves applying the simple exponential model known as Beer's law [30, 31].

$$f = 1 - exp(-K \times LAI), \quad LAI = d \times l, \quad l = F \times w. \tag{2.5}$$

2.2.2. Modeling plant growth in interaction with soil nutrients

In the context of one dimensional growth without branching, Bessonov–Volpert have conceptualized the growing plant as a vertical interval, hence we consider the interval $0 \le z \le L(x)$ where the bottom endpoint is fixed at $z = 0$ and the top endpoint is denoted as $z = L(x)$ (Fig. 1).

The growth mechanism is based on many assumptions:

1) Nutrients enter at $z = 0$ and are transported upward through the interval via convective and diffusion fluxes.

$$\frac{\partial C}{\partial x} + u\frac{\partial C}{\partial z} = d\frac{\partial^2 C}{\partial z^2} \tag{2.6}$$

here d is the diffusion coefficient, and u is the velocity of the fluid.

2) The growing part of the plant where cells divide is called the meristem located at the top of the plant. Cell division and growth are controlled by external signals called growth and mitosis signals. We will not distinguish between these two and we will call them for brevily GM-factors.
They are produced in meristem by the equation:

$$h\frac{\partial R}{\partial x} = g(R)C - \sigma R \tag{2.7}$$

$$\begin{cases} \frac{dL}{dx} = f(R) \\ u = \frac{dL}{dx} \\ \frac{\partial C}{\partial x} + u\frac{\partial C}{\partial z} = d\frac{\partial^2 C}{\partial z^2} \quad z \in]0, \mathrm{L}[\\ \mathrm{z} = 0 \quad : \quad \mathrm{C} = 1 \\ z = L(x) \quad : \quad d\frac{\partial C}{\partial z} = -g(R)C \\ h\frac{\partial R}{\partial x} = g(R)C - \sigma R \\ L(x=0) = L_0, \quad C(z,0) = C_0, \quad R(L = L_0) = R_0 \end{cases} \tag{11}$$

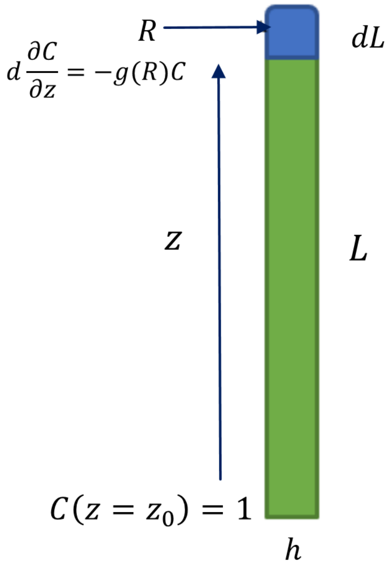

FIGURE 1. Schematic representation of the developed mathematical model in the case of 1D without branching.

where R is the concentration of GM-factor, h meristem's width, σ a parameter, and g a function well described in [20].

3) Completing equation (2.6) with boundary conditions. Assuming that the dimensionless concentration C varies between 0 and 1:

$$\mathrm{z} = 0 : \mathrm{C} = 1 \qquad z = L(x) : d\frac{\partial C}{\partial z} = -g(R)C \tag{2.8}$$

4) Assuming the fluid is incompressible and fills the stem uniformly, we obtain:

$$u = \frac{\mathrm{d}L}{\mathrm{d}x} \tag{2.9}$$

5) The value L increases with x (x=time, DD or EDD), the growth rate is determined by the concentration R. Thus

$$\frac{\mathrm{d}L}{\mathrm{d}x} = f(R) \tag{2.10}$$

where f is a piecewise constant function detailed in [21].
To complete our model, we need to incorporate the initial conditions. Therefore, our complete model can be written as follows:

2.2.3. *Combining models describing plant growth under varying environmental conditions with Bessonov–Volpert model*

In this section, we will utilize our previously fitted models to modify the Bessonov–Volpert system 1D without branching and describe plant growth under varying environmental conditions. While our models have characterized the average dry weight growth per plant, the Bessonov–Volpert model describes the growth in plant length. Therefore, it is necessary to establish a relationship between dry weight and plant length.

TABLE 2. Parameters and definitions used in the model (11).

Notation	Description	Value	Unit	References
C	Nutrient's concentration			[20]
R	Concentration of GM-factor,			[20]
L	Plant length		su	[20]
$C_0, R_0 L_0$	Initials conditions			
u	Velocity of the fluid	0.0003075	su/tu	Calibration
f	f is a piecewise constant function describing plant growth rate			[19, 20]
g	A function describing he production of the growth factor R			equation (3.3)
z	Space		su	
t	Time		tu	
σ	A parameter describing the consumption of R	0.009	su/tu	[21]
h	Width of meristem	0.05	su	Calibration
d	Diffusion coefficient	0.001	su^2/tu	[21]

su: Space unity.
tu: Time unity.

Suppose that the relationship between plant dry weight and length plant can be expressed by a simple allometric equation in the sense of Hexley [32]:

$$w = pL^q. \tag{2.11}$$

Here L is the length plant and p and q are constants.
This relationship was applied to lettuce plants and yielded good results as reported by Nagashima and Terashima [33].
By differentiating both sides of the equation (2.11) to x, we obtain;

$$\frac{\mathrm{d}w}{\mathrm{d}x} = pq\frac{\mathrm{d}L}{\mathrm{d}x}L^{q-1} \tag{2.12}$$

Now, let's consider the derivative forms of our growth models:

$$\text{Logistic:} \qquad \frac{1}{w}\frac{\mathrm{d}w}{\mathrm{d}x} = r\left(1 - \frac{w}{k}\right) \tag{2.13}$$

$$\text{Gompertz:} \qquad \frac{1}{w}\frac{\mathrm{d}w}{\mathrm{d}x} = c\ln\left(\frac{k}{w}\right) \tag{2.14}$$

$$\text{Aikman \& Scaife:} \qquad \frac{\mathrm{d}w}{\mathrm{d}x} = \frac{r}{dKF}\,(1 - exp(-dKFw)). \tag{2.15}$$

Then, we can combine the allometric equation with each of our models, by substituting (2.13), (2.14), and (2.15) in (2.12). This will give us the expression for L in terms of x for each model, we obtain:

$$\text{Logistic:} \qquad \frac{1}{L}\frac{\mathrm{d}L}{\mathrm{d}x} = r'\left(1 - \frac{L^q}{k'^q}\right) \tag{2.16}$$

$$\text{Gompertz:} \qquad \frac{1}{L}\frac{\mathrm{d}L}{\mathrm{d}x} = c\ln\left(\frac{k'}{L}\right) \tag{2.17}$$

$$\text{Aikman \& Scaife:} \qquad \frac{1}{L}\frac{\mathrm{d}L}{\mathrm{d}x} = r'\,\phi' \tag{2.18}$$

where;

$$\phi' = \frac{1 - exp(-nKFpL^q)}{nKFpL^q}, \qquad r' = \frac{r}{q}, \qquad k' = L_{max}.$$

Since the previously adjusted models have demonstrated a great ability to describe the growth of plant dry weight under varying environmental conditions, and the Bessonov- Volpert model describes the growth of plant length without considering the impact of environmental conditions, we can combine the Bessonov–Volpert model with the previously adjusted models by describing the growth of plant length in terms of effective day-degrees (x=EDD) instead of chronological time (x=t). Additionally, we can modify the expression of the function f by assuming that the growth rate is no longer constant. Specifically, for values of R less than R_0, the growth rate is set to zero, and for values of R between R_0 and R_1, the growth rate follows the modified expressions given by (2.16), (2.17), or (2.18).

3. RESULTS

3.1. Calibration of models' parameters

3.1.1. Logistic model

Figure 2A shows the observed values of dry weight plotted against time from sowing using the logistic function for different densities which are 180, 480, 1920, and 7680 plants per m^2. The values of k and r, which represent carrying capacity and relative growth rate, respectively, varied largely between experiments.

In Figure 2B, chronological time was substituted for thermal time, giving the best fit to a straight line in the figures, resulting in a reduction in the amount of scatter. The growth rates varied between experiments, and it was observed that the growth rate for plants sown in the spring was much higher than that of plants sown in other seasons. This is likely due to light, so a new scale was sought that included the effect of light as well as temperature.

Scaife *et al.* [14, 34] proposed a new factor that describes the interaction between temperature and radiation, which is effective day-degrees (EDD).
The expression of EDD is:

$$EDD_i^{-1} = DD_i^{-1} + f \times R_i^{-1} \quad \text{where} \quad DD_i = \sum_{k=1}^{i} max(0, T_k - T_0) \tag{3.1}$$

where T_k is the temperature of kth day, DD_i is the conventional day-degrees total for the ith day (above T_0), R_i is the total PAR ($\mathrm{MJ\,m^{-2}}$) for the ith day, and f is a parameter denoting the importance of light vis-a-vis temperature. The value of T_0 was given as $T_0 = 3.5$ [14].

Figure 2C demonstrates the impact of replacing time with effective day-degree, as the results for all experiments at a particular density now appear highly consistent and closely overlapping.

Table 3 presents the optimal values of parameters w_0, k, r, and f for the logistic model. The coefficient of determination (R^2) is also provided, indicating the goodness of fit using these optimal values. The results

TABLE 3. Parameter estimates for the logistic model using EDD for different densities.

Model	d	w_0	k	r	f	R^2
Logistic	180	0.00034439	1.87564838	0.02442168	0.10687613	99.98%
	480	0.00050975	1.09293809	0.02275224	0.11651107	99.96%
	1920	0.00098824	0.37608501	0.01913844	0.14602330	99.72%
	7680	0.00149904	0.13670291	0.01447856	0.20415953	99.03%

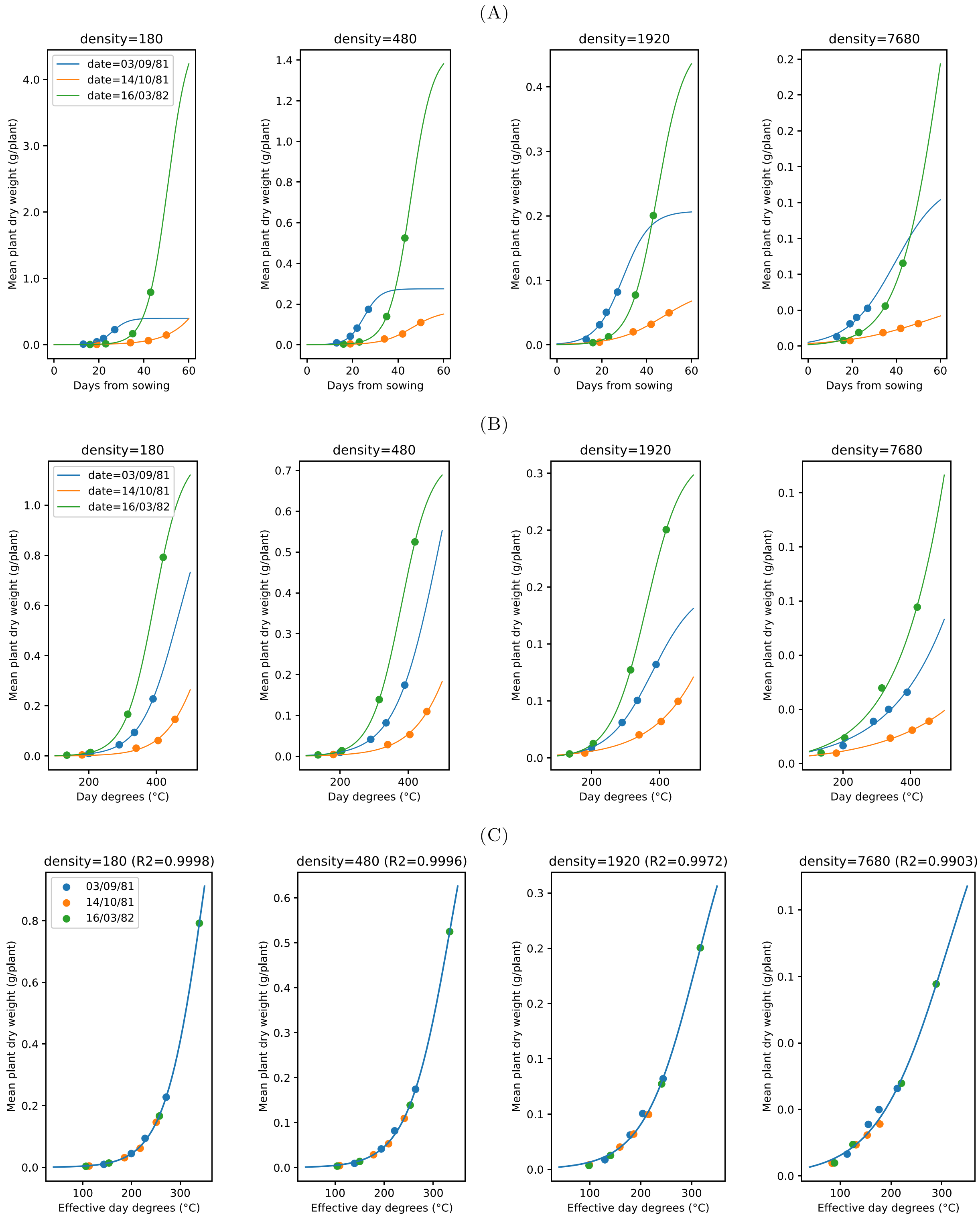

FIGURE 2. Fit of the logistic model to observed mean dry weight using time from sowing (A), day-degrees (B), and effective day-degrees (C) at different densities and sowing dates.

TABLE 4. Parameter estimates for the Gompertz model using EDD for different densities.

Model	d	a	b	c	f	R^2
Gompertz	180	167.08584455	15.24267172	0.00308760	0.10756124	99.98%
	480	26.31353823	12.93764967	0.00359084	0.11775442	99.97%
	1920	2.51345940	9.27436980	0.00412407	0.15006972	99.80%
	7680	1.04017079	7.00996029	0.00309337	0.21145675	99.14%

demonstrate that the logistic model with EDD is highly suitable for modeling plant growth under different planting densities, with R^2 values exceeding 99% for all densities.

As shown in Table 3, an interesting trend emerges as the plant density increases. The relative growth rate decreases, indicating a reduction in the rate of growth per unit of EDD. Additionally, the carrying capacity, represented by parameter k, also decreases with increasing density. These observations strongly suggest that competition for resources, such as radiation, plays a significant role in shaping plant growth patterns. The decrease in carrying capacity implies that as density increases, plants face greater limitations in accessing essential resources, leading to reduced growth potential.

3.1.2. Gompertz function

Table 4 presents the parameter estimates for the Gompertz model using EDD for different planting densities. Similar to the logistic model, the Gompertz model demonstrates excellent performance in modeling plant growth, with R^2 values exceeding 99% for all densities.

Comparing the results of the Gompertz model to those of the logistic model, a similar trend emerges. As the plant density increases, the growth rate, represented by parameter c, decreases. This suggests that the rate of growth per unit of EDD becomes slower under higher planting densities. Additionally, the carrying capacity, represented by parameter a, also decreases with increasing density. These findings further support the notion that competition for resources, including radiation, is a key factor influencing plant growth patterns.

Furthermore, it is interesting to note that the coefficient of determination R^2 for the Gompertz model follows a similar pattern as the logistic model, with a decrease in predictive power as density increases. If we divide the graph of the logistic model into three parts, the first part represents the exponential growth phase, followed by the maturation phase where the relative growth rate starts to decline, and finally, the saturation phase where the carrying capacity is reached. In both the logistic and Gompertz models, we observe that the data points lie in the exponential growth phase and the maturation phase but do not reach the saturation phase. This could potentially be attributed to the specific characteristics of our crop, which requires a longer time to reach its carrying capacity, and the harvests in our experiments were conducted at an earlier stage, contributing to the absence of data points in the saturation phase. The same reason has led to a wide variation in the value of a in the Gompertz model; this issue could be addressed with more data, providing a more comprehensive representation of the growth phases and enabling better parameter estimation.

3.1.3. Aikman and Scaife model

Aikman & Scaife developed a model under varying environmental conditions (has as analytical solution (2.3), based on Goudriaan & Monteith function [10], this model is based on a continuous smooth expolinear function. In their model, the slope of the linear phase that follows the exponential growth phase is related to the earlier exponential growth rate r.

Table 5 presents the optimal values of parameters f_0, f, KF, r, and R^2 for the Aikman and Scaife model.

Upon examining the results, we observe a similar trend as in the previous models. As the planting density increases, the relative growth rate and the coefficient of determination decrease.

TABLE 5. Parameter estimates for the Aikman & Scaife model using EDD in equation for different densities.

Model	d	f_0	f	KF	r	R^2
Aikman & Scaife	180	0.00045155	0.10698924	0.00781957	0.02481226	99.98%
	480	0.00118687	0.11668077	0.00542550	0.02340976	99.96%
	1920	0.00718936	0.14734754	0.00449016	0.02040752	99.74%
	7680	0.03093226	0.20678644	0.00295530	0.01540276	99.06%

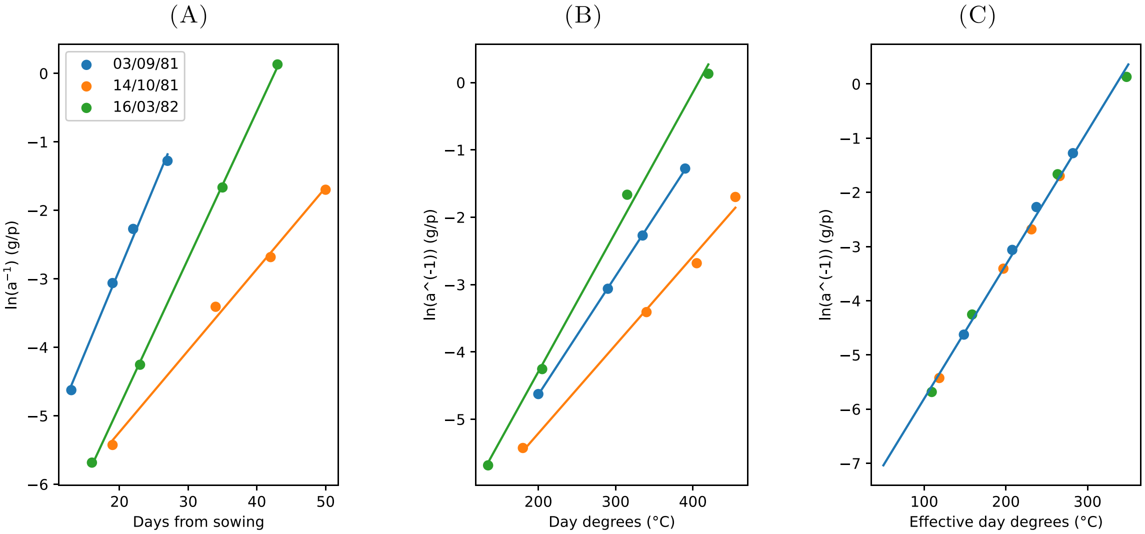

FIGURE 3. Relationship between $\ln(a^{-1})$ and time from sowing (A), day-degrees (B), and effective day-degrees (C).

3.1.4. Scaife, Cox and Morris model

Scaife, Cox, and Morris further developed the model proposed by Scaife and Jones (1976) [12] by incorporating the following Shinozaki-Kira equation [35]:

$$w^{-1} = a + b \times d \tag{3.2}$$

where w ($\mathrm{g\,p^{-1}}$) mean dry weight per plant and d is plant density ($\mathrm{p\,m^{-2}}$).
As d → 0, w → a^{-1}, hence a^{-1} represents the weight of an isolated plant ($g\,p^{-1}$).
If d → ∞, wd → b^{-1}, hence b represents the reciprocal of yield per m^2 ($\mathrm{m^2\,g^{-1}}$).
To derive the expressions for a and b, Scaife, Cox & Morris relied on the suggestion put forth by Scaife & Jones [12] for the expression of a, stating that the weight of an isolated plant a^{-1} follows an exponential growth pattern. As for b^{-1}, it is linearly dependent on the radiation received during the 14 days prior to harvest (MDR).

$$a^{-1} = w_0\,\mathrm{e}^{rx} \qquad\qquad b^{-1} = q\;MDR.$$

Figure 3A displays the relationship between the natural logarithm of a^{-1} and the time from sowing. The slopes and intercepts differ among the three experiments, indicating variations in growth patterns. To reduce variability, in Figure 3B, we replaced chronological time with thermal time, resulting in a more compact distribution of data points. However, the lines representing different experiments still show some deviation. To achieve better

TABLE 6. Parameter estimates for Scaife, Cox & Morris model using EDD for different densities.

Model	w_0	p	f	q^{-1}	T_0	R^2 for expression of		
						a	b	$w^{-1} = a + b\,d$
Scaife, Cox & Morris	0.0002558	0.02466	0.0934	0.00925745	3.5	99.67%	-36.19%	90.74%

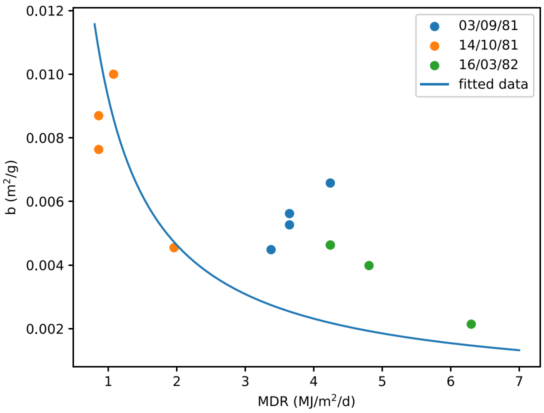

FIGURE 4. Relationship between b and mean PAR for the 14 days before harvest.

alignment, we introduced the concept of effective day-degrees in Figure 3C, which significantly improved the overlap of results across all sowings.

Unlike the previous models, the model incorporates the density variable, eliminating the need to determine optimal parameters for each density.

Table 6 presents the coefficient of determination of ln w^{-1} explained by effective day-degrees (C), and the relationship between the ceiling yield b^{-1} and MDR. The table also includes the optimal values of w_0, p, f, q, and T_0.

For the expression of b, a hyperbolic relationship was used instead of a linear relationship, to avoid obtaining unrealistic results (see Fig. 4).

One particular value of parameter b, which was negative, was excluded from the analysis due to its susceptibility to significant errors.

The coefficient of determination for the Scaife, Cox & Morris model is 90.74%, which is significantly lower compared to the other models that have coefficients of determination exceeding 99% for all four densities. This difference is attributed to the improper expression of parameter b (–36.19%).

3.2. Numerical simulations

In our numerical simulations, we employed constant values for several parameters to ensure the consistency of our calculations. These constants include: d=0.001$\frac{su}{tu^2}$, σ=0.009$\frac{su}{tu}$, h=0.05su, $g_0 = 0.01\frac{su}{tu}$, Rg_1=0.01, Rf=0.04, Rg_2=1, L_0=0.1su, R_0=1, C(x,0)=1, p=0.41$\frac{g}{su}$, and q= 3.3 where su is space unity and tu time unity.
The functional form of g(R) is described by the following piecewise function:

$$g(R) = \begin{cases} \frac{g_0}{Rg_1} R, & \text{si } 0 \leq R \leq Rg_1 \\ g_0, & \text{si } Rg_1 \leq R \leq Rg_2 \\ 0, & \text{sinon} \end{cases}. \tag{3.3}$$

For each equation in the system, we employed specific numerical methods.

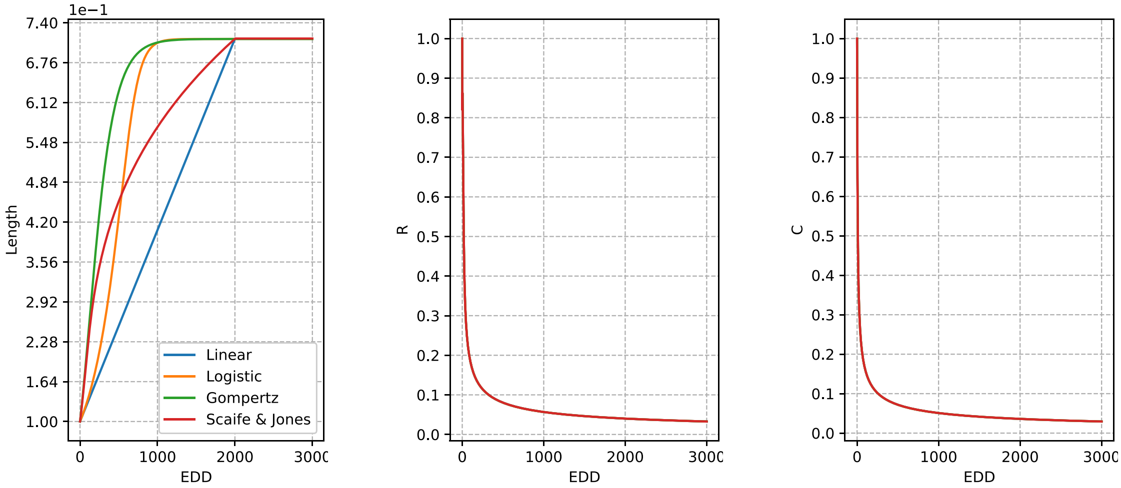
(A) Plant stem length growth L vs. EDD (B) Metabolite Concentration R vs. EDD (C) Nutrients Concentration C at end point vs. EDD

FIGURE 5. Growth of stem length (A) with corresponding changing of the concentrations of metabolites (B) and nutrients concentration (C) at apex using linear, logistic, Gompertz and Scaife & Jones model.

TABLE 7. Parameters used for linear, logistic, Gompertz and Scaife & Jones model in Figures 5 and 6.

Linear		Logistic		Gompertz		Scaife & Jones		
f_0	k	r	k	c	k	r	KF	n
0.0003075	0.714	0.01	0.135	0.0055	0.135	0.033	0.59	800

For equation (2.6) describing the variation of C, we utilized the Crank-Nicolson method with $h_t = 10^{-4}$tu, $h_x = 10^{-3}$su,. We applied the explicit Euler method for (2.7), (2.8) and (2.10) describing respectively the variation of R, boundary condition for C and L.

We envision a virtual plant placed in a plot with a given density, having a maximum capacity of 0.714 su. Therefore, Figure 5A illustrates the different growth trajectories that the plant can follow in terms of length, using equations (2.16), (2.17), and (2.18).

Figures 5B, 5C depict the variation of R and C as a function of effective day-degrees ($0 \leq EDD \leq 3000$). The curves closely overlap, making it difficult to discern the differences in the C and R variations for each model. To address this, in Figure 6B, we have plotted the variation of C for each model in comparison to the linear model, represented as $|C(i) - C_L(i)|$ where $C(i)$ is the concentration of the considered model when EDD = i, $C_L(i)$ is the concentration of the linear model when EDD=i. The same approach was applied to R (6A).

Table 7 presents the parameter values utilized in Figure 5, where the growth curves for different models are depicted. These values were chosen to ensure equality in the maximum length for all models, resulting in clear and comparable growth patterns. Notably, the carrying capacity value k for the weight parameter is set to 0.135, calculated using equation (2.11) as: $0.41 \times (0.714^{3.3}) = 0.135$. Each parameter value is carefully selected to accurately represent the growth characteristics of the respective model.

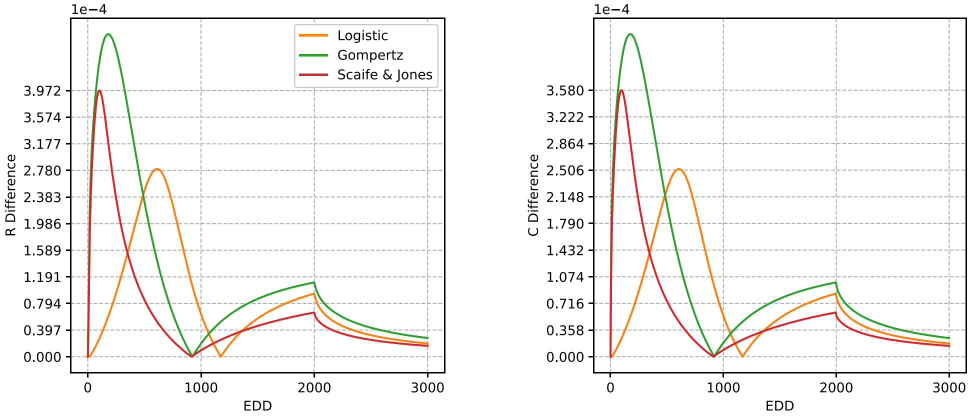
(A) (B)

Figure 6. Deviation of Metabolite Concentration C (A) and growth factor Concentration R (B) from the linear model across different EDD values.

4. Discussion and conclusion

4.1. Comparison between the four models

In this study, we examined the growth patterns of lettuce plants under variable environmental conditions. By using different growth models, we were able to estimate the growth parameters and assess the impact of time, day-degrees, and effective day-degrees on plant growth at different densities.

Furthermore, incorporating the concept of effective day-degrees significantly improved the alignment of results across different sowings, indicating the importance of accounting for the cumulative effects of temperature and radiation on plant growth. This approach allowed us to characterize the growth of plant weight under varying environmental conditions, providing valuable insights into the response of lettuce plants to different densities and seasonal variations.

We observed that as the density increased, the coefficient of determination (R^2) decreased for all three models: logistic, Gompertz, and Aikman & Scaife. For example, the R^2 value for the logistic model at density $d = 180$ was 99.98%, while for density $d = 7680$, it decreased to 99.03%. Similar trends were observed for the Gompertz and Aikman & Scaife models, where the R^2 values decreased as the density increased.

Figure 7 illustrates the observed weights plotted against the estimated weights for each model at different densities. We can observe that for all three models, the estimated weights are in close agreement with the observed weights for density $d = 180$. However, as we move to higher densities (*e.g.*, $d = 1920$), we can see slight deviations in the estimated weights, indicating either underestimation or overestimation. Nevertheless, the discrepancy remains negligible across all three models.

For the Scaife, Cox & Morris model (Fig. 8), replacing chronological time with effective day-degrees improved the overlap of results across all sowings for the four densities for the description of the growth of isolated plant weight. However, it should be noted that the improper expression of parameter b had a negative impact on the model's performance. and then, we did not integrate this model into the Bessonov–Volpert model.

4.2. Numerical simulations: Exploring model predictions and performance

Numerical simulations of the Bessonov–Volpert model reveal two distinct growth modes, termed linear and oscillating. The linear mode occurs when $Rg_1 < R_f$, while the oscillating mode prevails when $Rg_1 > R_f$. In our

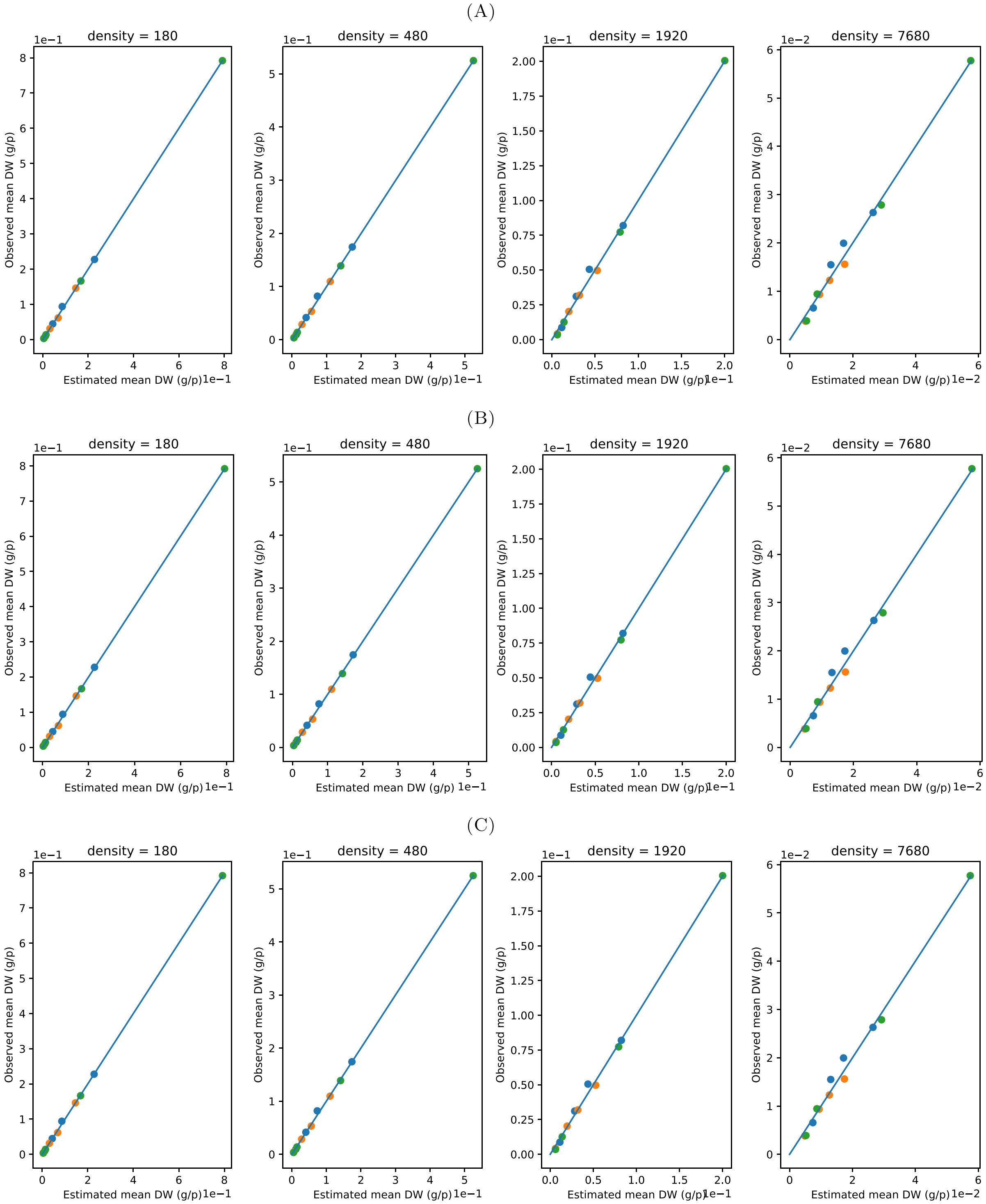
(A)

(B)

(C)

FIGURE 7. Observed values of mean dry weight (DW) against values predicted by logistic (A), Gompertz (B), and Aikman & Scaife (C) functions for different densities using effective day-degrees.

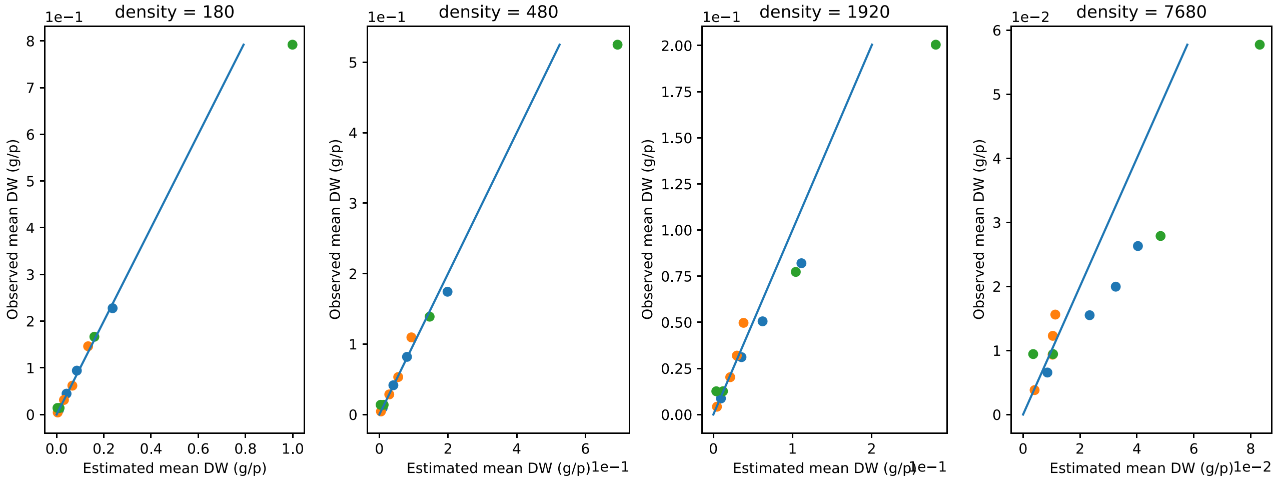

FIGURE 8. Observed values of dry weight against values predicted by the Scaife, Coxt & Morris model for different densities using effective day-degrees.

investigation, we specifically focused on the scenario where $Rg_1 < R_f$ by adjusting the plant's growth rate using (2.16), (2.17), and (2.18).

In plots with a given density, the growth trajectory cannot adhere to linearity due to shading among plants. Consequently, the model predicts an almost exponential growth before shading, but over time, the growth rate diminishes. Figure 5A delineates diverse growth scenarios for a plant within a plot, revealing variations in growth rates among different models. Referring to (2.7) and (2.8), which depict the variations in C and R at the apex, a higher growth rate correlates with a swifter decline in concentrations of C and R.

Upon scrutinizing Figure 5, considering the parameters specified in Table 7, we observe that during the early growth phase, the Scaife & Jones model exhibits the highest growth rate, succeeded by the Gompertz model, the logistic model, and, ultimately, the linear model.

Transitioning to Figure 6, clear oscillations are apparent, undoubtedly influenced by the diverse growth rates among the different models. However, generally, this variation did not have a pronounced effect on the fluctuations of R and C between the models.

In summary, our study aimed at developing a robust mathematical model to comprehensively describe plant growth, considering both environmental conditions and soil nutrient availability. The initial exploration involved the analysis of lettuce plants in a field experiment, incorporating various growth models such as logistic, Gompertz, Aikman & Scaife, and Scaife, Cox & Morris.

The integration of effective day-degrees proved pivotal, enhancing model accuracy and allowing a more nuanced understanding of plant growth under varying environmental conditions. Notably, the substitution of chronological time with effective day-degrees in the Bessonov–Volpert system equations provided a more accurate representation of one dimensional plant weight growth.

Moving forward, our investigation expanded into numerical simulations of the Bessonov–Volpert model, revealing distinct growth modes influenced by varying growth rates. Notably, the Scaife & Jones model exhibited the highest early growth rate.

In conclusion, this study lays the foundation for a comprehensive model that encapsulates the intricate interplay between environmental conditions and soil nutrients in plant growth. As we move forward, further refinements, validations against empirical data, and the consideration of additional environmental factors will be essential for advancing our understanding of crop growth dynamics. This work contributes to the broader goal of developing sustainable agricultural practices in the face of changing environmental conditions.

APPENDIX A.

TABLE A.1. Sowing and harvest dates of each experiment of lettuce, PAR, MDR, and values of a^{-1} and b^{-1} from the equation of Shinozaki-Kira $w^{-1} = a + bd$.

Crop	Expt sowing date	Harvest dates	$a^{-1}(g)$	$b^{-1}(\mathrm{g\,m^{-2}})$	PAR(MJ $\mathrm{m}^{-2}d^{-1}$)	MDR(MJ m^{-2})
Lettuce	03/09/1981	16/09	0.0098	152	4.15	4.242
		22/09	0.0468	178	2.42	3.646
		25/09	0.1032	190	2.55	3.646
		30/09	0.2789	223	3.82	3.377
	14/10/1981	02/11	0.0044	220	1.70	1.96
		17/11	0.0331	100	0.75	1.077
		25/11	0.0684	115	0.83	0.86
		03/12	0.1829	131	1.17	0.86
	16/03/1982	01/04	0.0034	-207	3.34	4.242
		08/04	0.0142	216	1.73	4.242
		20/04	0.1891	251	7.05	4.807
		28/04	1.1398	467	4.84	6.3

DATA AVAILABILITY STATEMENT

The source codes for all the results mentioned in this article are available on GitHub at the following link: https://github.com/HassanChini/MultiScaleHybridModeling [36].

REFERENCES

[1] R.J. Hanks and V.P. Rasmussen, Predicting crop production as related to plant water stress. *Adv. Agron.* **35** (1982) 193–215.

[2] J.E. Newman, Symposium: responses of field crops to environmental factors summary statements. *Agron. J.* **55** (1963) 31–31.

[3] J.F. Farrar and M.L. Williams, The effects of increased atmospheric carbon dioxide and temperature on carbon partitioning, source-sink relations and respiration. *Plant Cell Environ.* **14** (1991) 819–830.

[4] P. Stiling and T. Cornelissen, How does elevated carbon dioxide (co2) affect plant–herbivore interactions? A field experiment and meta-analysis of co2-mediated changes on plant chemistry and herbivore performance. *Global Change Biol.* **13** (2007) 1823–1842.

[5] N.M. Crawford, Nitrate: nutrient and signal for plant growth. *Plant Cell* **7** (1995) 859.

[6] Z. Wang and S. Li, Effects of nitrogen and phosphorus fertilization on plant growth and nitrate accumulation in vegetables. *J. Plant Nutr.* **27** (2004) 539–556.

[7] D.P. Aikman and L.R. Benjamin, A model for plant and crop growth, allowing for competition for light by the use of potential and restricted projected crown zone areas. *Ann. Bot.* **73** (1994) 185–194.

[8] A. Barnes, The influence of the length of the growth period and planting density on total crop yield. *Ann. Bot.* **41** (1977) 883–895.

[9] L.R. Benjamin and D.P. Aikman, Predicting growth in stands of mixed species from that in individual species. *Ann. Bot.* **76** (1995) 31–42.

[10] J. Goudriaan and J.L. Monteith, A mathematical function for crop growth based on light interception and leaf area expansion. *Ann. Bot.* **66** (1990) 695–701.

[11] H.J.W. Mutsaers, A dynamic equation for plant interaction and application to yield-density-time relations. *Ann. Bot.* **64** (1989) 521–531.

[12] M.A. Scaife and D. Jones, The relationship between crop yield (or mean plant weight) of lettuce and plant density, length of growing period, and initial plant weight. *J. Agric. Sci.* **86** (1976) 83–91.

[13] D.P. Aikman and A. Scaife, Modelling plant growth under varying environment conditions in a uniform canopy. *Ann. Bot.* **72** (1993) 485–492.

[14] A. Scaife, E.F. Cox and G.E.L. Morris, The relationship between shoot weight, plant density and time during the propagation of four vegetable species. *Ann. Bot.* **59** (1987) 325–334.

[15] F. Tei, D.P. Aikman and A. Scaife, Growth of lettuce, onion and red beet. 2. growth modelling. *Ann. Bot.* **78** (1996) 645–652.

[16] F. Tei, A. Scaife and D.P. Aikman, Growth of lettuce, onion, and red beet. 1. Growth analysis, light interception, and radiation use efficiency. *Ann. Bot.* **78** (1996) 633–643.

[17] S.A. Barber, Soil Nutrient Bioavailability: A Mechanistic Approach. John Wiley & Sons (1995).

[18] F.J. Molz, Models of water transport in the soil-plant system: A review. *Water Resources Res.* **17** (1981) 1245–1260.

[19] T. Roose and A. Schnepf, Mathematical models of plant–soil interaction. *Philos. Trans. Roy. Soc. A: Math. Phys. Eng. Sci.* **366** (2008) 4597–4611.

[20] N. Bessonov and V. Volpert, Dynamical models of plant growth. Mathematics Subject Classification (2000).

[21] N. Bessonov, F. Crauste and V. Volpert, Modelling of plant growth with apical or basal meristem. *Math. Model. Natural Phenomena* **6** (2011) 107–132.

[22] J.P. Baldwin, P.B. Tinker and P.H. Nye, Uptake of solutes by multiple root systems from soil: II. The theoretical effects of rooting density and pattern on uptake of nutrients from soil. *Plant Soil* **36** (1972) 693–708.

[23] L. Dupuy, P.J. Gregory and A.G. Bengough, Root growth models: towards a new generation of continuous approaches. *J. Exp. Bot.* **61** (2010) 2131–2143.

[24] R. Pearl and L.J. Reed, Skew-growth curves. *Proc. Natl. Acad. Sci. U.S.A.* **11** (1925) 16–22.

[25] P.-F. Verhulst, Notice sur la loi que la population suit dans son accroissement. *Correspondence Math. Phys.* **10** (1838) 113–129.

[26] B. Gompertz, On the nature of the function expressive of the law of human mortality, and on a new mode of determining the value of life contingencies. in a letter to francis baily, esq. frs &c. by benjamin gompertz, esq. fr s, In *Abstracts of the Papers Printed in the Philosophical Transactions of the Royal Society of London.* The Royal Society London (1833) 252–253.

[27] D.P. Aikman, Tuning and validation illustrated by a model of plant competition. In: The art and craft of modelling in applied biology. *Asp. Appl. Biol.* **26** (1991) 122–134.

[28] A.G. Bengough, Modelling rooting depth and soil strength in a drying soil profile. *J. Theor. Biol.* **186** (1997) 327–338.

[29] D.J. Greenwood, T.J. Cleaver, S.M.H. Loquens and K.B. Niendorf, Relationship between plant weight and growing period for vegetable crops in the United Kingdom. *Ann. Bot.* **41** (1977) 987–997.

[30] M.A.P. de León and B.N. Bailey, Evaluating the use of Beer's law for estimating light interception in canopy architectures with varying heterogeneity and anisotropy. *Ecol. Model.* **406** (2019) 133–143.

[31] M. Monsi, The light factor in plant communities and its significance for dry matter production. *Jap. J. Bot.* **14** (1953) 22.

[32] J.S. Huxley, Problems of Relative Growth. Dial Press, New York (1932).

[33] H. Nagashima and I. Terashima, Relationships between height, diameter and weight distributions of chenopodium album plants in stands: effects of dimension and allometry. *Ann. Bot.* **75** (1995) 181–188.

[34] A. Scaife, R.A. Sutherland et al., A new photothermal growth unit: the 'ffective day-degree', in *First Congress of the European Society of Agronomy.* European Society of Agronomy (1990).

[35] K. Shinozaki, Intraspecific competition among higher plants. VII. Logistic theory of the cd effect. *J. Biol. Osaka City Univ.* **7** (1956) 35–72.

[36] H. Chini, Python code for "Multi-Scale Hybrid Modeling of Plant Growth in Response to Environmental Conditions and Soil Nutrients Availability" (2024). https://github.com/HassanChini/MultiScaleHybridModeling